OnLine Journal of Earth Sciences 1 (3): 154-162, 2007
ISSN: 1991-7708

Numerical Simulation of a Wind-Sand Flow

Ping Lü and Zhibao Dong
Key Laboratory of Desert and Desertification, Cold and Arid Regions Environmental and Engineering Research Institute, Chinese Academy of Sciences, Lanzhou, Gansu 730000, PR China

Abstract: A theoretical model for wind-sand flow is developed by consideration of coupling among wind flow, sand particle motion and the Magnus effect under different atmospheric stability conditions. Using this model, the characteristics of the movement of wind and sand in the wind-sand flow are discussed in detail. The results show that the atmospheric stability and the Magnus effect both have a strong effect on wind profiles and on the trajectories of sand particles and that these effects produce results with different characteristics from those previously reported in the study, which apply only to neutral stability: The saltating sand reaches a greater height under non-neutral stability than under neutral stability, while the maximum horizontal distance is higher under unstable conditions and is smaller under stable conditions than under neutral stability.

Key words: Atmospheric stability, magnus effect, wind profile, numerical simulation

INTRODUCTION

The wind-sand flow is a kind of two-phase (gas-solid) turbulent fluid movement that occurs within the atmospheric turbulent boundary layer (Zhu *et al*., 2001). This flow is an issue of central importance in the physics of blown sand and thus, is of central importance in developing basic theories of aeolian sand landforms, desertification and wind sand control engineering. The focus of this two-phase flow is the interaction between the wind and the sand particles; that is, the sand is affected by the wind, meanwhile, the moving sand also has retardatory effects on the wind. This coupled interaction between the wind and saltating particles leads to so-called "self-regulating feedback mechanism" in wind-sand flow. That is to say, for a specific reference wind velocity, the movement of wind-blown sand will attain an equilibrium state when the number of moving sand grains and the resulting sand transport rate reach a certain value and the wind profile will subsequently remain stable (Bagnold, 1941; Owen, 1964; Ungar and Haff, 1987; Anderson and Haff, 1991; Huang and Zheng, 2003, 2006; Zheng *et al*., 2003, 2006).

Systematic studies of the wind-sand flow can be dated back to the 1930s and began with field observations and experimental studies (Bagnold, 1935, 1936, 1941; Chepil, 1951; Owen, 1964). Several scholars and experts began to study the characteristics of the wind-sand flow using numerical simulation after the symposium on the physics of blown sand held in the Aarhus University, Denmark in 1985 (Anderson, 1987; Ungar and Haff, 1987; Anderson and Haff, 1988, 1991; Werner, 1990; McEwan and Willitts, 1991, 1993; Haff and Anderson, 1993; Spies *et al*., 2000; Leenders *et al*., 2005). Ungar and Haff (1987) proposed a single-way theoretical model by considering the mutual coupling interaction between wind flow and sand movement. This model relied on the description of a stable 2-D wind-sand saltation. However, the model used a simplification that assumed identical motion for all sand particles; that is, it assumed that every sand particle hits the sand bed and lifts another particle and that all the sand particles jump vertically from the sand bed at the same speed. In addition, the equation for sand motion in this model only accounted for gravity and aerodynamic drag. Therefore, even though the model represented a conceptual breakthrough at the time, it is too simplistic. In addition to the effects of gravity and drag, the movement of sand particles is also affected by the Magnus effect created by the rotation of the moving sand (Chepil, 1951; White and Schulz, 1977) and they found that the sand particles are in high speed rotation for the collision among them during their saltation movement by means of experiment. White and Schulz (1977) simulated the influence of the Magnus effect on the trajectories of saltating sand particles using a numerical model. Their results indicated that the Magnus effect exerts a significant influence on the trajectories of sand particles and can increase the height of sand motion by 20%. However, they did not consider the counterforce exerted by the sand on the wind, therefore, their numerical model cannot be one for a coupling model.

In addition, past research only focused on the neutral atmospheric stability (i.e., the temperature of the air equals that of the earth's-surface and does not change

Corresponding Author: Ping Lü, Key Laboratory of Desert and Desertification, Cold and Arid Regions Environmental and Engineering Research Institute, Chinese Academy of Sciences, Lanzhou, Gansu 730000, PR China

with height, the clean wind profile obeys the rule of the wall) and they ignored the influence of thermal factors (i.e., changes in the temperature of the earth's-surface and the atmosphere) and the vertical wind velocity produced by the thermal factors. Previous studies suggested that the strong solar radiation in gobi and desert of the arid and semi-arid areas creates variability in the temperature of the earth's surface and of the atmosphere in the boundary layer and that this temperature gradient has an obvious influence on the flow strength in the boundary layer and on the particle concentration in the saltation layer (Liu, 1960; Zhang *et al*., 2004). Under different stability conditions, the temperature gradient and the wind profile obey different laws. Under the unstable conditions, the surface temperature is higher than that of the atmosphere above that surface and this difference generates a kind of upward buoyancy, that reinforces the wind intensity within the turbulent boundary layer (Stull, 1988; Cai *et al*., 2002; Liu *et al*., 2002; Hu *et al*., 2004; Zhang *et al*., 2004). Under this condition, the clean wind profile can be demonstrated by a concave-upward curve on the semi-logarithmic coordinate. Under the stable conditions, the surface temperature is lower than that of the atmosphere above the surface and this difference generates a vertical downward buoyancy, that restrains the wind intensity in the turbulent boundary layer (Stull, 1988; Cai *et al*., 2002; Liu *et al*., 2002; Hu *et al*., 2004; Zhang *et al*., 2004) and the clean wind profile can be illustrated by a convex-upward curve under the semi-logarithmic coordinate. Under the neutral condition, the atmospheric temperature doesn't change with height and no buoyancy effect occurs, thus the effect of temperature can be ignored in models. So far as the interaction between wind and sand is concerned, under non-neutral conditions, the trajectories of moving sand particles and the wind profile will change correspondingly with the change in wind intensity and in the temperature gradient. In order to thoroughly understand the characteristics of the wind-sand flow, we cannot emphasize only dynamical factors in our models; we must also pay careful attention to thermal factors.

Based on the analysis above, we developed a theoretical simulation model that considers both the effects of dynamic factors and the effects of thermal factors. By means of numerical simulation, we describe the trajectories of moving sand and the wind profiles under non-neutral conditions and discuss their important differences between neutral and non-neutral stability cases.

THE MOTION EQUATIONS FOR SALTATING SAND PARTICLES

For simplicity, we have assumed that the sandy surface is composed of spherical grains with identical diameter, D_p and that m_p is the mass of a sand particle. Consider a 2-D rectangular Cartesian coordinate system with x and z axes in which the motion of the sand is steady, the x-axis represents the horizontal direction parallel to the wind flow and the positive z-axis represents the vertical direction above the sand bed. By accounting for the effective gravitational force, the drag force exerted by the wind and the Magnus effect, the motion equations for saltating sand particles can be written as follows (White and Schulz, 1977):

$$m_p\frac{d^2x}{dt^2}=-\frac{1}{8}\rho\pi D_p^2\left(\frac{24\gamma}{D_p\sqrt{(\dot{x}-u)^2+(\dot{z}-w)^2}}+\frac{6.0}{1+\sqrt{D_p\sqrt{(\dot{x}-u)^2+(\dot{z}-w)^2}/\gamma}}+0.4\right)\times(\dot{x}-u)\sqrt{(\dot{x}-u)^2+(\dot{z}-w)^2}+\frac{1}{8}\rho\pi D_p^3(\dot{z}-w)\left(\dot{\theta}-\frac{1}{2}\frac{\partial u}{\partial z}\right)$$

$$m_p\frac{d^2z}{dt^2}=-\frac{1}{8}\rho\pi D_p^2\left(\frac{24\gamma}{D_p\sqrt{(\dot{x}-u)^2+(\dot{z}-w)^2}}+\frac{6.0}{1+\sqrt{D_p\sqrt{(\dot{x}-u)^2+(\dot{z}-w)^2}/\gamma}}+0.4\right)\times(\dot{z}-w)\sqrt{(\dot{x}-u)^2+(\dot{z}-w)^2}-m_pg-\frac{1}{8}\rho\pi D_p^3(\dot{x}-u)\left(\dot{\theta}-\frac{1}{2}\frac{\partial u}{\partial z}\right) \quad (1)$$

Where, x and z are the coordinates of sand particles, $\dot{x}$ and $\dot{z}$ are the sand velocity in the x and z directions,u and w are the wind velocity in the x and z directions, ρ is the air density, t is the time, γ is the coefficient of kinematical viscosity of air and θ is the sand particle's angular velocity.

THE NAVIER-STOKES EQUATION FOR WIND-SAND FLOW

After considering the interaction between the wind flow and the moving sand in the saltation layer, the effect of saltating particles on the air can be depicted by adding extra body force F in Navier-Stokes equation. So we can write the Navier-Stokes equation for the wind flow (White, 1974):

$$\rho\frac{\partial\vec{U}}{\partial t}+\rho(\vec{U}\cdot\nabla)\vec{U}=-\nabla P+\nabla\cdot\vec{\tau}-\rho g+\vec{F} \quad (2)$$

Where $\vec{U}$ is the wind velocity vector, P is the pressure of the air, $\vec{\tau}$ is the shear-stress tensor, $\vec{F}$ denotes the volume force per unit volume. As we known: the interaction between the wind and saltating particles leads to so-called "self-regulating feedback mechanism"

in wind-sand flow, so we can given steady ($\partial/\partial t = 0$) and horizontally uniform ($\partial/\partial z >> \partial/\partial x$) flow (Anderson and Haff, 1991; McEwan and Willitts, 1993), we can rewrite the equation as follows:

$$\rho w\frac{\partial u}{\partial z} = \frac{\partial \tau_{xz}}{\partial z} + F_x \tag{3.a}$$

$$\rho w\frac{\partial w}{\partial z} = -\frac{\partial p}{\partial z} + \frac{\partial \tau_{zz}}{\partial z} - \rho g + F_z \tag{3.b}$$

According to the Boussinesq assumption (Fu, 1995):

$$\tau_{ij} = \rho \cdot \nu_t\left(\frac{\partial u_i}{\partial x_j} + \frac{\partial u_j}{\partial x_i}\right) \tag{4}$$

That is:

$$\tau_{xz} = \rho \cdot \nu_t\frac{\partial u}{\partial z}, \tau_{zz} = 2\rho \cdot \nu_t\frac{\partial w}{\partial z}$$

Where, ν_t is the eddy viscosity. Under conditions of neutral and non-neutral stability, we use different parameterization for ν_t (Ungar and Haff, 1987; Shao and Lu, 1999).

Neutral stability: Under the condition of neutral stability, we adopt a popular and well-known one-and-half order parameterization scheme of turbulent kinetic energy (k) and the dissipation rate of turbulent kinetic energy (ε) (Shao and Lu, 1999) and this closure technique for turbulent modelling can give us more information about turbulent kinetic energy (k) and the dissipation rate of turbulent kinetic energy (ε):

$$\nu_t = 0.09\frac{k^2}{\varepsilon} \tag{5}$$

The equations for k and ε:

$$\frac{\partial k}{\partial t} + u_j\frac{\partial k}{\partial x_j} = \frac{\tau_{ij}}{\rho}\frac{\partial u_i}{\partial x_j} + \frac{\partial}{\partial x_j}\left(\frac{\nu_t}{\sigma_K}\cdot\frac{\partial k}{\partial x_j}\right) - \varepsilon \tag{6}$$

$$\frac{\partial \varepsilon}{\partial t} + u_j\frac{\partial \varepsilon}{\partial x_j} = \frac{C_{\varepsilon 1}}{\rho}\frac{\varepsilon}{k}\tau_{ij}\frac{\partial u_i}{\partial x_j} + \frac{\partial}{\partial x_j}\left(\frac{\nu_t}{\sigma_\varepsilon}\cdot\frac{\partial \varepsilon}{\partial x_j}\right) - C_{\varepsilon 2}\frac{\varepsilon^2}{k} \tag{7}$$

The reduced form for Eq. 6-7:

$$\frac{\partial k}{\partial t} + w\frac{\partial k}{\partial z} = \frac{\tau_{xz}}{\rho}\frac{\partial u}{\partial z} + \frac{\tau_{zz}}{\rho}\frac{\partial w}{\partial z} + \frac{\partial}{\partial z}\left(\frac{\nu_t}{\sigma_K}\cdot\frac{\partial k}{\partial z}\right) - \varepsilon$$

$$\frac{\partial \varepsilon}{\partial t} + w\frac{\partial \varepsilon}{\partial w} = \frac{C_{\varepsilon 1}}{\rho}\frac{\varepsilon}{k}\tau_{xz}\frac{\partial u}{\partial z} + \frac{C_{\varepsilon 1}}{\rho}\frac{\varepsilon}{k}\tau_{zz}\frac{\partial w}{\partial z} + \frac{\partial}{\partial z}\left(\frac{\nu_t}{\sigma_\varepsilon}\cdot\frac{\partial \varepsilon}{\partial z}\right) - C_{\varepsilon 2}\frac{\varepsilon^2}{k}$$

Where, σ_k, C_{c1}, C_{c2} and σ_c are constants with the values 1.0, 1.44, 1.92 and 1.3, respectively (Launder and Spalding, 1974). The air density can be derived from the continuity equation:

$$\frac{\partial \rho}{\partial t} + \frac{\partial(\rho U_j)}{\partial x_j} = 0 \tag{8}$$

Substituting Eq. 4 and 5 into Eq. 3, considering the temperature does not change with the height under neutral stability and thus, the buoyancy effects do not arise, we can only focus on the wind in the x direction, then we can get the equation under neutral stability:

$$\frac{\partial}{\partial z}\left(\rho \cdot 0.09\frac{k^2}{\varepsilon}\cdot\frac{\partial u}{\partial z}\right) = -F_x \tag{9}$$

Where, F_x is the horizontal body force per unit volume on the wind by the saltating sand particles.

Non-neutral stability: Under the condition of non-neutral stability, we adopt the prandlt's mixing-length (McEwan and Willitts, 1991):

$$\nu_t = l^2\frac{\partial U}{\partial z} \tag{10}$$

Where, l is the mixing-length, which changes as a result of dynamical and thermal factors. According to Liu *et al.* (1991):

$$l = Az^{1-e} \tag{11}$$

Where $A = kz_0^e$ and depends on the stability parameter e and on the surface roughness length z_0. Under unstable conditions:

$$-1 \prec e \prec 0 \tag{12}$$

The lower the value of, the greater the degree of instability. Under stable conditions:

$$0 \prec e \prec 1 \tag{13}$$

The higher the value of e, the greater the degree of stability.

Then:

$$l = kz\left(\frac{z}{z_0}\right)^{-e} \quad (14)$$

Where k is Von Karman's constant (k = 0.4).
Substituting (14) into Eq. 10:

$$\nu_t = k^2 z^2 \left(\frac{z}{z_0}\right)^{-2e}\left(\frac{\partial U}{\partial z}\right) \quad (15)$$

The temperature will change with height under the condition of the atmospheric instability and this generates the hot buoyancy that affects the vertical flow within the atmosphere. Therefore, we must consider not only the x direction of the wind, but also the z direction. Thus, we can get the equations of the wind under the non-neutral conditions:

$$\rho w\frac{\partial u}{\partial z} = \frac{\partial}{\partial z}\left[\rho k^2 z^2\left(\frac{z}{z_0}\right)^{-2e}\cdot\left(\frac{\partial u}{\partial z}\right)^2\right] + F_x \quad (16a)$$

$$\rho w\frac{\partial w}{\partial z} = -\frac{\partial p}{\partial z} + \frac{\partial}{\partial z}\left[\rho k^2 z^2\left(\frac{z}{z_0}\right)^{-2e}\cdot\left(\frac{\partial w}{\partial z}\right)^2\right] - \rho g + F_z \quad (16b)$$

Where:

$$F_x = -S\left[\frac{F_{Dx\uparrow}}{\dot{z}_\uparrow(z)} - \frac{F_{Dx\downarrow}}{\dot{z}_\downarrow(z)}\right] \quad (17a)$$

$$F_z = -S\left[\frac{F_{Dz\uparrow}}{\dot{z}_\uparrow(z)} - \frac{F_{Dz\downarrow}}{\dot{z}_\downarrow(z)}\right] \quad (17b)$$

(Ungar and Haff, 1987)

Where, S is the total number of sand particles ejected from the bed per unit area and unit time, on the assumption that the sand particles eject vertically from the sand bed at the same speed; the subscripts '↑' and '↓' represent ascending and descending particles, respectively; $\dot{z}_\uparrow$ and $\dot{z}_\downarrow$ are the vertical components of the velocity of ascending and descending sand grains at a given height and F_{Dz} and F_{Dz} are the drag forces on a single sand grain in the x and z directions, respectively. Above the sand saltation level, $F_x = 0$ and $F_z = 0$.

PARTICLE-BED IMPACTS

The interaction between saltating sand particles and the sand bed can be described using a so-called "splash function", $S(v_0, v_i)$, where S is the total number of sand particles ejected from the sand bed per unit area and unit time. For simplicity, we have employed a simple delta formula of splash function proposed by Ungar and Haff (1987):

$$S = A\frac{v_i^2}{D_p g}\delta^3\left(v_0 - B\frac{v_i^3}{D_p g}\right) \quad (18)$$

The meaning of Eq. (18) is that for a given impact velocity, v_i, there are those sand particles of number

$$A\frac{v_i^2}{D_p g}$$

ejected from the sand surface at the same vertical ejection velocity

$$B\frac{v_i^3}{D_p g}$$

For the condition of steady motion, we have,

$$A\frac{v_i^2}{D_p g} = 1 \text{ when } v_0 = B\frac{v_i^3}{D_p g}, \text{ further } vi = \sqrt{\frac{Dpg}{A}}$$

Where, A is a dimensionless constant that depends on the surface roughness, the shape of the sand, the friction between sand particles and the nature of the sandy surface.

SCHEME OF CALCULATIONS

The initial and boundary conditions for the model: In order to solve the nonlinear equations, we have defined the boundary conditions for Eq. 9 and 16 and the initial conditions for Eq. 1 and 6-8. The initial conditions are as follows:
t = 0:

$$x = 0, z = \frac{D_p}{30}, \dot{x} = 0, \dot{z} = v_0 \text{ and } \dot{\theta} = \dot{\theta}_0 \quad (19a)$$

$$k = 3\times10^{-3}U^2, \varepsilon = 0.09^{0.75}\times k^{1.5}/(kz), \rho = \rho_0 \quad (19b)$$

Here, v_0 is the vertical component of the initial velocity of the sand particle, θ_0 is the original rotation rate of the moving sand particle and $\rho_0 = 1.23$ kg m^{-3}.

For Eq. 9 and 16, the boundary conditions are as follows:
The lower boundary conditions:

$$z = D_p/30 : U = 0, \left\{\frac{\partial k}{\partial z}, \frac{\partial \varepsilon}{\partial z}, \frac{\partial \rho}{\partial z}\right\} = 0 \text{ and } \frac{dU}{dz} = c$$

Where, c is a constant to be adjusted. The upper boundary conditions:

$$w = 0, \left\{\frac{\partial k}{\partial z}, \frac{\partial \varepsilon}{\partial z}, \frac{\partial \rho}{\partial z}, \frac{\partial u}{\partial z}\right\} = 0$$

$$z \to \infty : u_* = kz\frac{dU}{dz} \text{(neutral condotion)}$$

$$z \to \infty : u_* = kz\left(\frac{z}{z_0}\right)^{-\varepsilon}\frac{dU}{dz} \text{(non-neutral condition)}$$

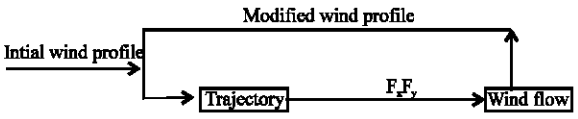

Fig. 1: Scheme of calculations used in the model

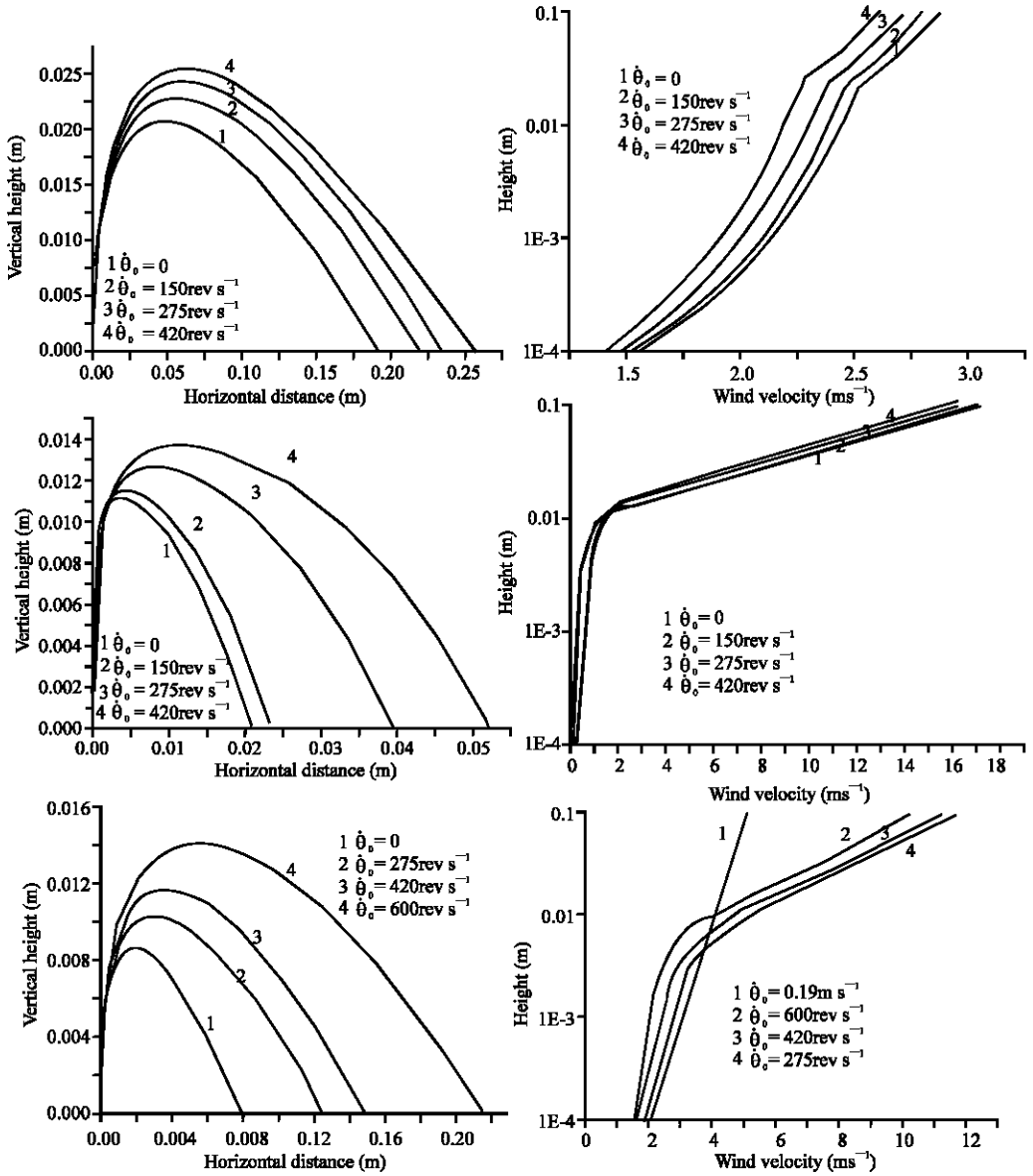

Fig. 2: Influence of the Magnus effect on the wind profiles and trajectories of blowing sand under different types of atmospheric stability

Calculation approach for the model: The main steps to solve the nonlinearly coupled equations can be seen from the literature of Zheng *et al.* (2003) and the calculation procedure for the model is illustrated in Fig. 1.

RESULTS AND DISCUSSION

The parameters of the sand grains used in this model are as follows:

$$\rho_g = 2650 kg m^{-3}, D_p = 0.25 mm$$

Influence of atmospheric stability and the Magnus effect upon saltation

Figuer 2 shows the influence of the Magnus effect on the wind profiles and trajectories of sand motion under three different stability conditions. It shows that the Magnus effect has a strong effect on the trajectories of sand particles for each form of stability and that the magnitude of the effect increases as the rotation rate of the particle increases. Take unstable situation for example, when the original rotation rate of the sand particle is zero, i.e. $\theta_0 = 0$, the horizontal distance and maximum height of the saltating sand particle are 190 and 20.6 mm, respectively, versus 217.9 and 22.8mm, respectively, at θ_0 = 150rev s^{-1}, 232.6 and 24.2 mm for θ_0 = 275rev s^{-1} and 255.1 and 25.4 mm for θ_0 = 420rev s^{-1}. As we known, the Magnus effect becomes greater In addition, Fig. 2 illustrates that the wind profile within the saltation layer shows remarkable difference from that at the outer saltation layer.

Figure 3 displays the effect of the different types of stability on the wind profile and trajectories of sand particles under rotation rates of θ_0 = 275 (top graphs) and 420 rev s^{-1} (bottom graphs). Figure 3 shows that the saltating sand reaches a greater height under non-neutral stability than under neutral stability, while the maximum horizontal distance is higher under unstable condition and is smaller under stable condition than under neutral stability. In addition, the wind profile is clearly different. For example, at θ_0 = 420 rev s^{-1}, the wind velocity at a height of 2 mm is 1.68 m s^{-1} under neutral condition, 1.98 m s^{-1} under instability and 0.7 m s^{-1} under stability.

Influence of the stability intensity upon saltation: The results presented above suggest that the atmospheric stability has a remarkable influence on the characteristics of the wind-sand movement. Figure 4 shows the influence of stability intensity with an original rotation rate θ_0 = 100 and 200 rev s^{-1}. In this fig., e is the stability index, with

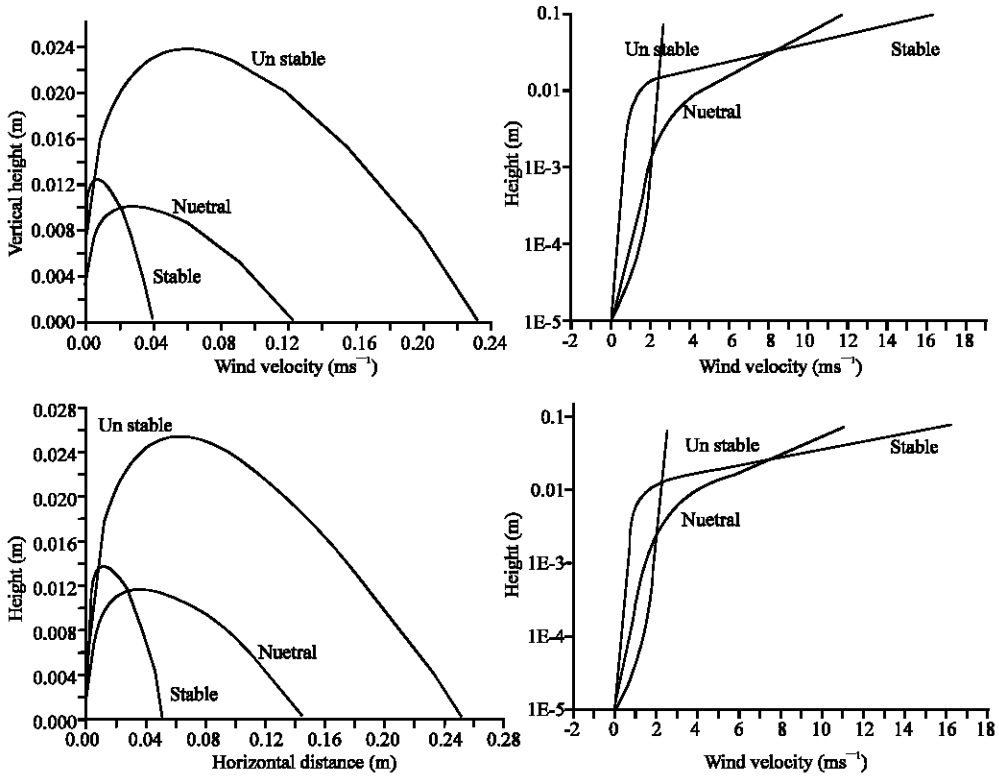

Fig. 3: Influences of atmospheric stability on the wind profiles and trajectories of saltating sand for two different original rotation spinning rates of the sand particles

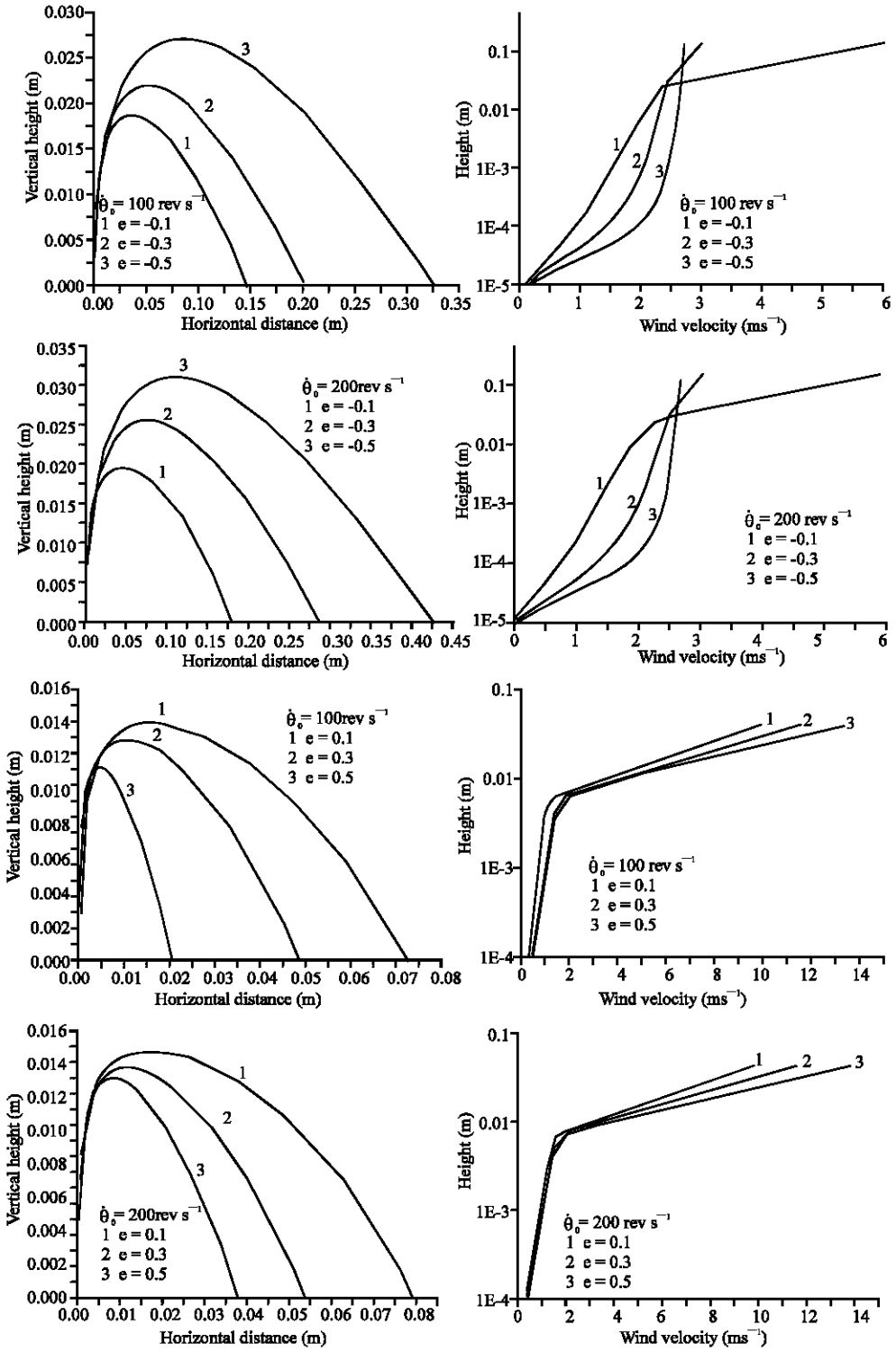

Fig. 4: Influences of stability intensity on trajectories of sand particles and on wind profiles

higher values of e (e > 0) representing increasing atmospheric stability. Figure 4 suggests that the stability strength has a noticeable effect on the wind profile and on the trajectories of sand particles. For example, under unstable conditions and $\dot{\theta}_0$ =100 rev s^{-1}, the horizontal distance and height of sand motion were 145.6 and 18.5

mm, respectively, for e = -0.1, versus 201 and 21.7 mm for e = -0.3 and 323.2 and 27.0 mm for e = -0.5. The results in Fig. 4 thus suggest that under unstable conditions, both maximum height and maximum horizontal distance increase with increasing stability intensity. Similarly, the wind profile shows obvious differences with respect to stability intensity.

Consequently, it is of great significance to carry on further study on the influence of different atmospheric stability, i.e. the effect of thermal factors.

CONCLUSION

In this study, we discuss the effects of thermal factors on the characteristics of a wind-sand flow by developing a theoretical model of the wind-sand flow that couples wind flow, the motion of sand particles and the Magnus effect under different atmospheric stability conditions. Our results show that the nature of the atmospheric stability (neutral, stable, or unstable), the degree of stability and the Magnus effect have strong effects on wind profiles and the trajectories of saltating sand particles: The maximum heights reached by sand particles under non-neutral condition are greater than those attained under neutral condition, whereas the maximum horizontal distance is greatest under unstable conditions and smallest under stable conditions. These results indicate dramatic differences with the results obtained under the assumption of neutral condition, which was the case in many previous studies. The Magnus effect also has a strong effect on the wind profiles and on the trajectories of saltating sand particles and the magnitude of the effect increased as the rotation rate increased. Our results indicate that it will be important to perform further studies of the characteristics of wind-sand movement under varying levels of atmospheric stability to improve our understanding of the mechanisms that govern soil erosion by the wind thoroughly.

In our study, we assumed a steady ($\partial/\partial t = 0$) flow, this assumption can not simulate the whole developing process of the wind-blown sand movement. Therefore we should perform further simulations on unsteady flow.

ACKNOWLEDGEMENT

We gratefully acknowledge the funding from the Knowledge Innovation Project of the Chinese Academy of Science (KZCX3-SW-341) and the National Science Fund for Distinguished Young Scholars of the Natural Science Foundation of China (40225003).

REFERENCES

Anderson, R.S., 1987. Eolian sediment transport as a stochastic process: The effects of a fluctuating wind on particle trajectories. J. Geol., 95: 497-512.

Anderson, R.S. and P.K. Haff, 1988. Simulation of eolian saltation. Science, 241: 820-823.

Anderson, R.S. and P.K. Haff, 1991. Wind modification and bed response during saltation of sand in air. Acta. Mech, 1: 21-25.

Bagnold, R.A., 1935. The movement of desert sand. Geographical J., 85: 342-369.

Bagnold, R.A., 1936. The movement of desert sand. Proc. Royal Soc. London, Series A, 154: 597-620.

Bagnold, R.A., 1941. The Physics of Blown Sand and Desert Dunes. Methuen, London, pp: 65.

Cai, X.H., F.T. Xie and J.Y. Chen, 2002. Large-eddy simulation for unstable surface layers. Acta Scientiarum Naturalium Universitatis Pekinensis, 38: 698-704.

Chepil, W.S., 1951. Properties of soil which influence wind erosion (part I to V). Siol. Sci., 71: 141-153.

Chepil, W.S. and N.P. Woodruff, 1963. The physics of wind erosion and its control. Adv. Agron., 15: 211-302.

Fu, S., 1995. Progress in the study of nonlinear turbulence modeling. Adv. Mechanics, 25: 318-328.

Haff, P.K. and R.S. Anderson, 1993. Grain scale simulation of loose sedimentary bed,the example of grain-bed impacts in aeolian saltation. Sedimentol., 40: 175-198.

Hu, Y.Q., S.F. Sun and Y.R. Zheng, 2004 Review of study on interaction between underlying surface with sparse vegetation and atmosphere. Plateau Meteorol., 24: 281-296.

Huang, N. and X.J. Zheng, 2003. Theoretical simulation of developing process of wind-blown sand movement. Key Eng. Mater., 243: 589-594.

Huang, N. and X.J. Zheng, 2006. The numerical simulation of the evolution process of wind-blown sand saltation and effects of electrostatical force. Chinese J. Theoretical Applied Mechanics, 38: 145-152.

Leenders, J.K., J.H. Boxel and G. Sterk, 2005. Wind forces and related saltation transport. Geomorphol., 71: 357-372.

Launder, B.E. and D.B. Spalding, 1974. The numerical computation of turbulent flows. Comput. Meth. Applied Mech. Eng., 3: 269-289.

Liu, S.H., Li, J. and P.H. Wen, 2002. Numerical simulation of atmospheric boundary-layer structure over urban and rural areas. Acta Scientiarum Naturalium Universitatis Pekinensis, 38: 90-97.

Liu, S.S. and S.D. Liu, 1991. The Atmospheric Dynamics. Peking University Publishers, Beijing, pp: 82.

Liu, Z.X., 1960. Transfer of sand in the surface layer. Acta Meteorologica Sinica, 31: 75-83.

McEwan, I.K. and B.B. Willetts, 1991. Numerical model of the saltation cloud. Acta Mech., Suppl., 1: 53-66.

McEwan, I.K. and B.B. Willetts, 1993. Adaptation of the near-surface wind to the development of sand transport. J. Fluid Mech., 252: 99-115.

Owen, P.R., 1964. Saltation of uniform grains in air. J. Fluid Mech., 20: 225-242.

Spies, P. J., McEwan, I. K. and R.B. Graeme, 2000. One-dimensional transitional behaviour in saltation. Earth Surface Process and Landforms, 25: 505-518.

Shao, Y. P. and A. Lu, 1999. Numerical modeling of saltation in the atmospheric surface layer. Boundary-layer Meteorol., 91: 199-225.

Stull, R.B., 1988 An Introduction to Boundary Layer Meteorology. Kluwer Academic Publishers, Boston, pp: 78.

Ungar, J. and P.K. Haff, 1987. Steady state saltation in air. Sedimentol., 34: 289-299.

Werner, B.T., 1990 A steady-state model of wind-blown sand transport. J. Geol., 1: 1-17.

White, F.M., 1974. Viscous Fluid Flow. McGraw-Hill Book Company, New York, pp: 32.

White, B.R. and J.C. Schulz, 1977. Magnus effect in saltation. J. Fluid Mech., 81: 497-512.

Zhang, Q., G.A. Wei and P. Hou, 2004. Observation studies of atmosphere boundary layer characteristic over Dunhuang gobi in early summer. Plateau Meteorol., 23: 587-597.

Zheng, X.J., N. Huang and Y.H. Zhou, 2003. Laboratory measurement of electrification of wind-blown sands and simulation of its effect on sand saltation movement. J. Geophys. Res., 108: 4322-4330.

Zheng, X.J., N. Huang and Y.H. Zhou, 2006. The effect of electrostatic force on the evolution of sand saltation cloud. Eur. Phys. J. E-Soft Matter, 19: 129-138.

Zhu, J.J., L.X. Qi and Z.B. Kuang, 2001. Velocity distribution of particle phase in saltating layer of wind-blowing-sand two phase flows. Acta. Mechanic Sinica, 33: 36-45.